

Reactions involved in the Heat Release and Pressure Wave Development during Autoignition of PRF/air Mixtures

Hsu Chew Lee¹, Peng Dai¹, Zheng Chen²

¹ Department of Mechanics and Aerospace Engineering, Southern University of Science and Technology, Shenzhen 518055, China

² SKLTCS, CAPT, BIC-ESAT, Department of Mechanics and Engineering Science, College of Engineering, Peking University, Beijing 100871, China

1 Introduction

Boosting technologies such as turbocharging are widely used in spark ignition engines (SIEs) due to their advantages of improved thermal efficiency and reduced fuel consumption. Unfortunately, further elevation of in-cylinder pressure in these advanced engines is constrained by knock and super-knock phenomena [1]. Specifically, reactivity non-uniformity in end gas is always inevitable and may induce localized autoignition and intense chemical-acoustic interactions. This may lead to knock or even super-knock, especially under boosted environment. Therefore, fundamental understanding of end-gas autoignition and accompanying pressure wave development under boosted engine conditions is needed.

After the pioneering work by Zel'dovich [2] who proposed different autoignition modes induced by reactivity non-uniformity, a number of studies have been conducted to extend his theory by theoretical analysis and numerical simulation [3-8]. Among them, Bradley and co-workers [4, 5] proposed a detonation peninsular induced by hot spot, using two non-dimensional parameters: the normalized temperature gradient, ζ , and the ratio of acoustic time to excitation time, ε . The detonation peninsular was widely utilized in the studies on knock and super-knock [9-11].

However, recent studies [6, 12-15] showed that the detonation regime in ζ - ε diagram quantitatively depends on the choice of fuels and chemical models. For example, Liberman and co-workers [15] found that the temperature gradient causing a detonation predicted by detailed chemical models greatly differs from that by one-step chemistry. Su et al. [14] investigated hot spot-induced autoignition in methane/air mixtures and observed notable discrepancies among the combustion modes using different kinetic models. In our recent studies [6, 7, 12], autoignition and detonation development of large hydrocarbon fuels with negative temperature coefficient (NTC) were investigated. It was found that the low-temperature chemistry greatly complicates the interaction between chemical reaction and pressure wave. Therefore, kinetic effects play a critical role in the autoignition process with reactivity non-uniformity and should be comprehensively investigated.

In the literature, there are few studies on the effect of detailed combustion chemistry on autoignition and interaction between chemical reaction and pressure wave [7, 11, 14]. The chemical reaction dominates the heat release process and therefore imposes great influence on local pressure pulse and its propagation.

Therefore, the objectives of this study are: (1) to identify the key elementary reactions affecting the ignition heat release properties in primary reference fuel (PRF)/air mixtures, and (2) to evaluate the kinetic effects on the localized autoignition and accompanying pressure wave development.

2 Model and specifications

In this study, the PRF blends consisting of n-heptane and iso-octane are considered. The skeletal mechanism [16] with 171 species and 861 reactions is used in simulations. Its performance in terms of describing autoignition and flame propagation has been well demonstrated [16].

The kinetic effects on the autoignition process are first examined in a 0D homogeneous constant-volume configuration. Their relevance in localized autoignition is then investigated by considering a reactive region of stoichiometric PRF/air mixture with radius r_0 , which is surrounded by inert gas (i.e. pure nitrogen), at the center of a 1D, adiabatic, closed, spherical chamber with radius $R_w=4$ cm. The interface between the reactive region and inert gas is characterized by the concentration distribution:

$$c_k(r) = \frac{c_{k,f} + c_{k,n}}{2} - \frac{c_{k,f} - c_{k,n}}{2} \tanh\left(\frac{r-r_0}{\delta}\right) \quad (1)$$

where c_k is the local concentration of the k th species and r_0 is the radius of the reactive region. The subscript f and n represent the stoichiometric PRF/air mixture and pure nitrogen, respectively. The parameter δ determines the width of the mixing layer and is set to be very small (i.e. 10^{-6}) in order to form a rather steep interface. The initial temperature T_0 and pressure P_0 are uniform within the chamber.

The 1D transient autoignition process is simulated using the in-house code A-SURF [17] which solves the conservation equations of 1D, compressible, multi-component, reactive flow using the finite volume method. A multi-level, dynamically adaptive mesh is used to maintain adequate numerical resolution of the reaction zone, pressure wave, shock wave, and detonation wave. The finest mesh size covering them is $0.4 \mu\text{m}$ and the corresponding time step is 0.02 ns.

3 Results and Discussion

0D homogeneous constant-volume ignition in stoichiometric PRF/air mixtures of three compositions (i.e., pure n-heptane, 50% n-heptane and 50% iso-octane in volume, and pure iso-octane) is first investigated. Figure 1 shows the ignition delay time, τ_{ig} , and excitation time, τ_e , which are respectively defined as the time of maximum heat release rate and the duration between 20% of the maximum heat release rate. The NTC behavior in terms of τ_{ig} is observed at lower temperatures (say, below 1000 K), which is weakened at higher pressure. τ_{ig} is significantly reduced (up to three orders of magnitudes), while τ_e is less reduced (within one order of magnitude), with the increase of initial temperature. On the other hand, both τ_{ig} and τ_e are only slightly reduced (within one order of magnitude) with the increase of initial pressure.

Figure 2 shows the maximum heat release rate, q_{max} , during 0D ignition of different conditions and fuel compositions. It is seen that q_{max} is greatly enhanced by the elevation of pressure while less promoted by the increase of temperature. Besides, according to Figs. 1 and 2, increase of n-heptane blending in PRF leads to lower τ_{ig} and τ_e , and higher q_{max} . It is also noted that the variation trends of τ_e and q_{max} with changing temperature, pressure and fuel composition are always opposite to each other.

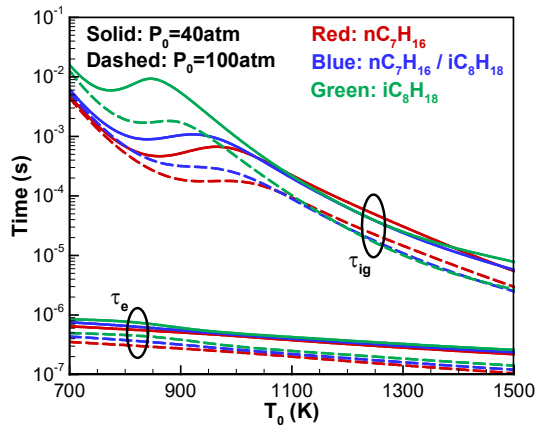


Fig. 1 Change of 0D ignition delay time and excitation time with initial temperature in stoichiometric PRF/air mixtures.

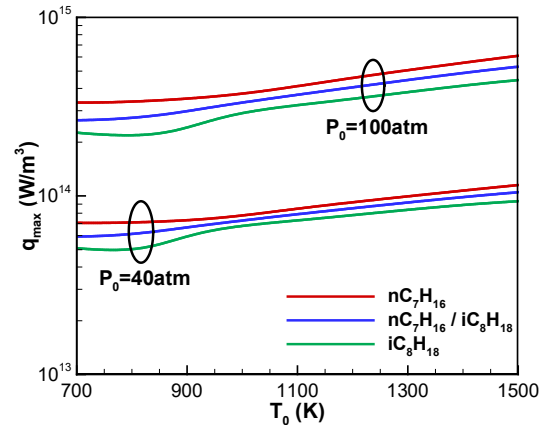


Fig. 2 Change of maximum heat release rate during 0D ignition with initial temperature in stoichiometric PRF/air mixtures.

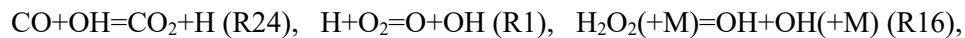
Since τ_e and q_{max} evaluate the rapidity and intensity, respectively, of the major heat release around ignition, they play critical roles in the local autoignition and accompanying pressure wave development [5, 11, 12]. On the other hand, τ_{ig} dominates the sequence of ignition events with non-uniform reactivity and its spatial variation may lead to different autoignition modes including detonation which is characterized by strong chemical-acoustic interactions [2]. Therefore, to identify the key elementary reactions involved in PRF/air autoignition, sensitivity analysis of τ_{ig} , τ_e and q_{max} is conducted. The sensitivity coefficient of the excitation time with respect to the reaction rate of the i th elementary reaction is defined as:

$$S_{e,i} = \frac{\tau_e(2K_i) - \tau_e(K_i)}{\tau_e(K_i)} \quad (2)$$

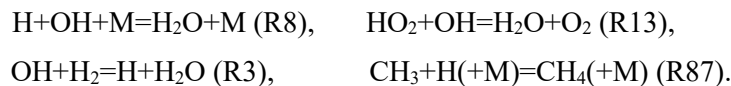
where $\tau_e(2K_i)$ represents the excitation time when the rate constant of the i th elementary reaction is artificially modified to be 2 times of its original value (K_i). A negative (positive) value of $S_{e,i}$ indicates that the rapidity of ignition heat release is promoted (inhibited) by the i th elementary reaction. The definitions of sensitivity coefficients of τ_{ig} and q_{max} (i.e. $S_{ig,i}$ and $S_{q,i}$) are similar to that of $S_{e,i}$. The results of sensitivity analysis of τ_e are plotted in Fig. 3.

According to Fig. 3, the key reactions controlling the rapidity of ignition heat release include:

Promoting reactions:



Inhibiting reactions:



Among them, the influence of R24, R8, R13, R16 and R3 on τ_e is shown to decrease, while that of R87 increases, with the increase of initial temperature. The effects of R8, R13 and R16 increase while that of R87 decreases with the increase of initial pressure. Besides, the influence of R1 is hardly affected by the variation of temperature and pressure. The sensitivity analysis of q_{max} (details are not shown here due to space limit) identifies the same key reactions and similar variation trends, except that $S_{q,i}$ always has an opposite sign to corresponding $S_{e,i}$. This is consistent with the observation in Figs. 1 and 2 that q_{max} changes oppositely with τ_e . It is noted that reactions involved in low-temperature chemical path, which result in NTC behavior, have negligible effect on τ_e and q_{max} . This indicates that the intense heat release around ignition is hardly affected by the low-temperature chemistry of PRF fuels.

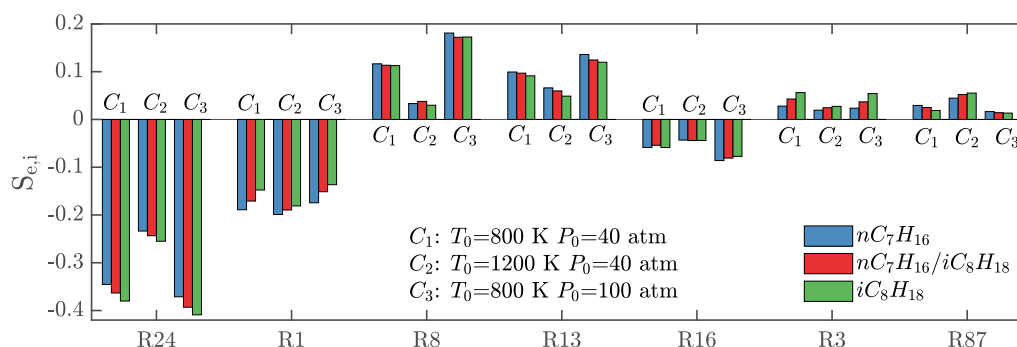
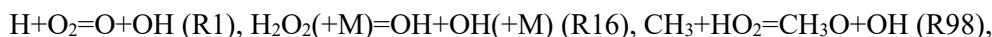


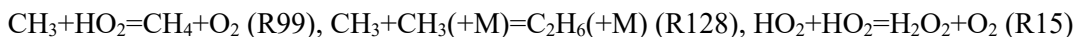
Fig. 3 Sensitivity coefficients of excitation time with respect to key elementary reactions during 0D ignition in stoichiometric PRF/air mixtures.

The sensitivity analysis of τ_{ig} (details are not shown here) identifies the following key reactions dominating the ignition delay:

Promoting reactions:



Inhibiting reactions:



where RH, R, RO_2 , and $\text{R}'\text{OOH}$ represent $n\text{C}_7\text{H}_{16}/i\text{C}_8\text{H}_{18}$, $\text{C}_7\text{H}_{15}/\text{C}_8\text{H}_{17}$, $\text{C}_7\text{H}_{15}\text{O}_2/\text{C}_8\text{H}_{17}\text{O}_2$, and $\text{C}_7\text{H}_{14}\text{O}_2\text{H}/\text{C}_8\text{H}_{16}\text{O}_2\text{H}$, respectively, X denotes radicals including OH, HO_2 , H, etc. As expected, the effects of low-temperature chemistry including LTR1 and LTR2 on ignition delay are significantly inhibited by increasing initial temperature, which makes the corresponding sensitivity coefficients approach zero. Besides, it is found that R1, R98, R99 and R128 have minor influence on τ_{ig} at low temperature and pressure (e.g. $T_0=800\text{K}$ and $P_0=40\text{atm}$) while they greatly affects τ_{ig} at high temperature (e.g. $T_0=1200\text{K}$) or pressure (e.g. $P_0=100\text{atm}$).

The sensitivity analysis of τ_e , q_{max} and τ_{ig} reveals that the elementary reactions controlling the intensity of ignition heat release are not exactly the same as those dominating the ignition delay. Only R1 and R16 have great effects on both ignition heat release and ignition delay, which significantly reduce τ_{ig} and τ_e and increase q_{max} in the same time. The low-temperature chemistry hardly affects the ignition heat release although it greatly influences the ignition delay and causes NTC behavior at low temperature. Therefore, the kinetic mechanism dominating the intense ignition heat release partly differs from that controlling the ignition delay, both of which play critical roles in the autoignition with reactivity non-uniformity.

The 1D autoignition process of PRF/air reactive region surrounded by nitrogen is simulated at different conditions. Figure 4 shows the temporal evolution of temperature and pressure profiles for a typical case. It is seen that the temperature increases uniformly within the reactive region (i.e., $r \leq r_0$) during autoignition. On the other hand, the pressure at the center of the reactive region (i.e. the left boundary of the computation domain) rises faster than outer locations. After ignition (i.e. $t > \tau_{ig}$), the pressure within the reactive region decreases rapidly and a pressure wave with a decreasing peak propagates into the inert gas (see lines 9-12 in Fig. 4). It is noted that the maximum pressure achieved within the reactive region (i.e. $P_{max}=104.5$ atm as shown in Fig. 4) is much lower than the equilibrium value of homogeneous constant-volume ignition (i.e. $P_e=296$ atm). This is mainly due to the outwardly propagation of pressure pulse and expansion of the reactive region.

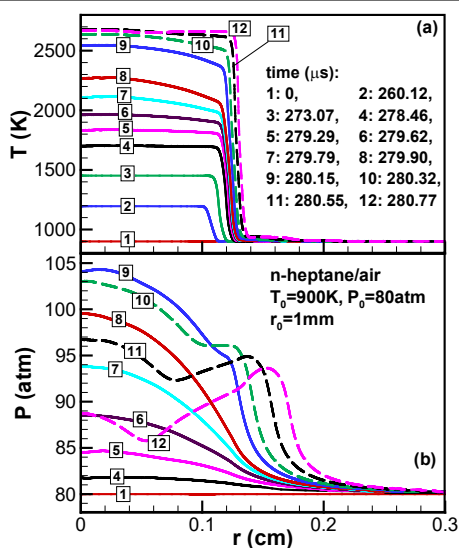


Fig. 4 Temporal evolution of (a) temperature and (b) pressure distribution during autoignition of n-heptane/air reactive region with $r_0=1\text{mm}$.

Since τ_e dominates the rapidity of ignition heat release, it is expected to have great effect on P_{max} of local reactive region. Figure 5 summarizes the maximum pressure during autoignition in n-heptane/air and iso-octane/air reactive regions. P_{max} and τ_e are normalized by initial pressure P_0 and τ_e of n-heptane/air at $T_0=1200\text{K}$ and $P_0=100\text{atm}$, respectively. It is seen that the normalized maximum pressure decreases with increasing excitation time. Besides, the curves of different fuel compositions and initial conditions collapse into one other at given r_0 . This indicates that the excitation time dominates the pressure pulse of local reactive region at varying PRF compositions and conditions. Therefore, the autoignition and accompanying pressure wave development are significantly influenced by both the kinetic mechanisms controlling τ_{ig} and those dominating τ_e and q_{max} . In addition, P_{max}/P_0 increases with r_0 in Fig. 5 and is expected to achieve the equilibrium value of homogeneous constant-volume ignition when r_0 approaches infinity.

4 Conclusions

The kinetic effects involved in autoignition of PRF/air mixtures are numerically investigated considering detailed chemistry. It is found that increase of initial temperature, initial pressure, and blending ratio of n-heptane in PRF can all promote the ignition heat release, which is manifested by a reduction of excitation time and increase of maximum heat release rate. Key elementary reactions affecting the excitation time, maximum heat release rate, and ignition delay are identified through sensitivity analysis. It is found that the kinetic mechanism dominating ignition heat release is partly different from that controlling ignition delay, both of which play critical roles in autoignition with reactivity non-uniformity. Autoignition of stoichiometric PRF/air reactive region surrounded by inert gas is simulated for various fuel compositions and initial conditions. The outwardly propagation of pressure pulse and expansion of the reactive region during autoignition are observed. Therefore, the maximum pressure achieved within the reactive region is much lower than the equilibrium value of homogeneous constant-volume ignition. The maximum pressure at different fuel compositions and conditions is summarized in a $P_{max}/P_0-\tau_e/\tau_{e,0}$ diagram. It is observed that the curves quantitatively agree with one another at given r_0 , indicating that excitation time dominates the pressure pulse within local reactive region. Therefore, the autoignition and accompanying pressure wave development are significantly influenced by the reactions controlling ignition delay, excitation time and maximum heat release rate.

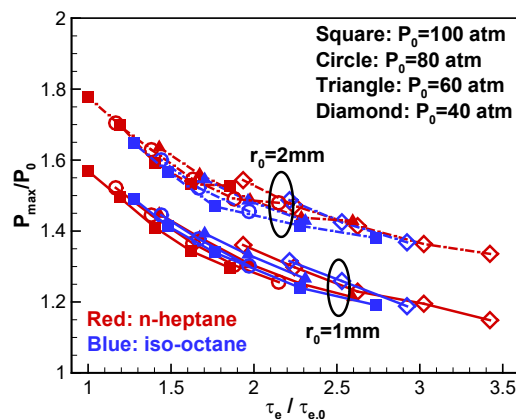


Fig. 5 Change of the maximum pressure, P_{max} , normalized by the initial value, P_0 , with the excitation time, τ_e , normalized by the value of n-heptane/air at $T_0=1200\text{K}$ and $P_0=100\text{atm}$, $\tau_{e,0}$.

Acknowledgements

This work is supported by National Natural Science Foundation of China (Nos. 51976088 and 92041001).

References

- [1] Wang Z, Liu H, Reitz RD. (2017). Knocking combustion in spark-ignition engines. *Prog. Energy Combust. Sci.* 61: 78.
- [2] Zeldovich YB. (1980). Regime Classification of an Exothermic Reaction with Nonuniform Initial Conditions. *Combust. Flame* 39: 211.
- [3] Sharpe GJ, Short M. (2003). Detonation ignition from a temperature gradient for a two-step chain-branching kinetics model. *J. Fluid Mech.* 476: 267.
- [4] Bradley D, Morley C, Gu XJ, Emerson DR. (2002). Amplified pressure waves during autoignition: relevance to CAI engines. SAE Technical Paper, 2002-01-2868,
- [5] Gu XJ, Emerson DR, Bradley D. (2003). Modes of reaction front propagation from hot spots. *Combust. Flame* 133: 63.
- [6] Dai P, Qi CK, Chen Z. (2017). Effects of initial temperature on autoignition and detonation development in dimethyl ether/air mixtures with temperature gradient. *Proc. Combust. Inst.* 36: 3643.
- [7] Dai P, Chen Z. (2019). Effects of NO_x addition on autoignition and detonation development in DME/air under engine-relevant conditions. *Proc. Combust. Inst.* 37: 4813.
- [8] Zander L, Tornow G, Klein R, Djordjevic N. Knock Control in Shockless Explosion Combustion by Extension of Excitation Time. *Active Flow and Combustion Control 2018*. Cham: Springer International Publishing 151.
- [9] Kalghatgi GT, Bradley D. (2012). Pre-ignition and 'super-knock' in turbo-charged spark-ignition engines. *Int. J. Engine Res.* 13: 399.
- [10] Rudloff J, Zaccardi JM, Richard S, Anderlohr JM. (2013). Analysis of pre-ignition in highly charged SI engines: Emphasis on the auto-ignition mode. *Proc. Combust. Inst.* 34: 2959.
- [11] Bates L, Bradley D, Gorbatenko I, Tomlin AS. (2017). Computation of methane/air ignition delay and excitation times, using comprehensive and reduced chemical mechanisms and their relevance in engine autoignition. *Combust. Flame* 185: 105.
- [12] Dai P, Chen Z, Gan XH. (2019). Autoignition and detonation development induced by a hot spot in fuel-lean and CO₂ diluted n-heptane/air mixtures. *Combust. Flame* 201: 208.
- [13] Robert A, Zaccardi J-M, Dul C, Guerouani A, Rudloff J. (2018). Numerical study of auto-ignition propagation modes in toluene reference fuel–air mixtures: Toward a better understanding of abnormal combustion in spark-ignition engines. *Int. J. Engine Res.* 19: 1.
- [14] Su JY, Dai P, Chen Z. (2020). Detonation development from a hot spot in methane/air mixtures: Effects of kinetic models. *Int. J. Engine Res.*, doi:10.1177/1468087420944617
- [15] Wang C, Qian CG, Liu JN, Liberman MA. (2018). Influence of chemical kinetics on detonation initiating by temperature gradients in methane/air. *Combust. Flame* 197: 400.
- [16] Luong MB, Luo ZY, Lu TF, Chung SH, Yoo CS. (2013). Direct numerical simulations of the ignition of lean primary reference fuel/air mixtures with temperature inhomogeneities. *Combust. Flame* 160: 2038.
- [17] Chen Z, Burke MP, Ju YG. (2009). Effects of Lewis number and ignition energy on the determination of laminar flame speed using propagating spherical flames. *Proc. Combust. Inst.* 32: 1253.